Journal of Applied Fluid Mechanics, Vol. 9, No. 6, pp. 3147-3157, 2016.
Available online at www.jafmonline.net, ISSN 1735-3572, EISSN 1735-3645.

An analysis on Free Convection Cooling of a 3×3 Heater Array in Rectangular Enclosure using Cu-EG-Water Nanofluid

A. Purusothaman[1], V. Divya[2†], N. Nithyadevi[2], and H. F. Oztop[3]

[1] *Department of Mathematics, National Institute of Technology, Tiruchirappalli, India*
[2] *Department of Mathematics, Bharathiar University, Coimbatore, India*
[3] *Department of Mechanical Engineering, Technology Faculty, Firat University, Elazig, Turkey*

†*Corresponding Author Email: divya7291@gmail.com*

(Received February 3, 2016; accepted April 29, 2016)

ABSTRACT

This paper deals with the study of natural convection cooling of a discrete heater array in Cu-EG-water nanofluid filled rectangular enclosure. A 3 × 3 array of non-protruding heat sources is embedded on one of the vertical walls of the enclosure while the top horizontal and opposite vertical walls are assumed to be isothermally cold. The remaining portions in which the heaters are mounted and all other walls are insulated. The above setup is modeled into a system of partial differential equations which are solved numerically using finite volume method based on the Semi-Implicit Method for Pressure Linked Equation (SIMPLE) algorithm and power law scheme. The wide range of parameters for computation are the aspect ratio of the enclosure, the mixture proportion of Ethylene glycol-water, the solid volume fraction of the nanoparticle along with two different thermal conductivity models. It is observed that the proper choice of the computation parameters and thermal conductivity models could be able to maximize the heat transfer rate from the heater array. Also, the results obtained in this study will provide new guidelines in the field of electronic equipment cooling.

Keywords: Natural Convection; Equipment Cooling; Heater Array; Nanofluid; Thermal Conductivity

NOMENCLATURE

A_h	heater area
A_S	enclosure side aspect ratio
b	heater location
C	enclosure dimension in y direction
C_0	proportional constant
$C_{R,M}$	instantaneous velocity of the nanoparticle
C_P	constant pressure specific heat
d	diameter
D	enclosure dimension in x direction
D_0	microscopic diffusion coefficient
E	heater location
g	gravitational acceleration
H	enclosure dimension in z direction
k	thermal conductivity
l_m	free mean path of the base fluid
L_x, L_z	length and height of a heater
$Nu_{i,k}$	local Nusselt number of a heater
$\overline{Nu}_{i,k}$	average Nusselt number of a heater
$\overline{Nu}_i$	row averaged Nusselt number
p	pressure
P	dimensionless pressure
Pr	Prandtl number
Pr_T	thermal Rayleigh number
Ra	Rayleigh number
Re	Reynolds number
t	time
T	temperature
u,v,w	velocity components
U,V,W	dimensionless velocity components
x,y,z	cartesian coordinates
X,Y,Z	dimensionless cartesian coordinates
α	thermal diffusivity
β	thermal expansion coefficient
β_0	Kapitza resistance
μ	dynamic viscosity
ν	kinematic viscosity
ϕ	nanoparticle volume fraction
ρ	density
τ	dimensionless time
θ	dimensionless temperature
ζ	general variable

Subscripts

c	cold

f	fluid
h	hot
i	row
k	column
m	mixture
nf	nanofluid
p	nanoparticle

1. INTRODUCTION

A recent innovative technique for the enhancement of heat transfer rate using different forms of nanoparticles dispersed into a base fluid, known as nanofluid, has been studied extensively in the field of cooling the electronic devices. Nanofluid has many advantages over the basefluid because of anomalous increase of thermal conductivity. This is due to the Brownian motion exhibited by the nanoparticles and the nanoconvection occuring between the fluid molecules. The principal attempt on these newly engineered fluids was made by Choi and Eastman (1995) to demonstrate the production and potential benefits of nanofluids. Among the rheological properties, thermal conductivity is the most important characteristic to determine the heat transfer rate which motivates the researchers to examine the thermal conductivity behavior of nanofluids. Wang *et al*. (1999) used the steady-state parallel-plate technique to measure the thermal conductivity of nanofluids containing Al_2O_3 and CuO nanoparticles which were dispersed in water, ethylene glycol, vacuum pump oil and engine oil. However the theories failed to explain the anomalous increase of thermal conductivity behaviour which was illustrated in detail by Jang and Choi (2006). They explained the effects of various parameters such as the ratio of the thermal conductivity of nanoparticles to that of a base fluid, volume fraction, nanoparticle size and temperature on the effective thermal conductivity of nanofluids. Their comparison between the experimental and theoretical results archived excellent agreement and provided a new idea to the thermal scientists. A critical review has been done by Wang and Mujumdar (2007) and Trisaksri and Wongwises (2007) on the heat transfer characteristics of nanofluids to report the reason behind the enhancement of heat transfer while suspending nanoparticles into the conventional fluids. They suggested that the thermal conductivity is the key feature so that much attention was paid on the thermal conductivity rather than the heat transfer characteristics. Moreover, their study revealed that more clarification was needed to explain the thermal enhancement through the theoretical concept of nanofluids. In severe winter conditions, the need for fluids which can with-stand very low temperatures has motivated several authors to combine two different basefluids at a proper proportion. Namburu *et al*. (2007) presented an experimental investigation of rheological properties of copper oxide nanoparticles suspended in 60:40 (by weight) ethylene glycol and water mixture. It was found that the relative viscosity of copper oxide nanofluids was dependent on volume percentage and decreases substantially with temperature for higher concentrations. Lotfizadeh Dehkordi *et al*. (2013) focused the study on thermal conductivity and viscosity of alumina nanoparticles, at low volume concentrations of 0.01-1.0% dispersed in the mixture of ethylene glycol and water (mass ratio, 60:40). Sodiumdodeobcylbenzene sulfonate (SDBS) was applied for better dispersion and stability of alumina nanoparticles and found that SDBS at different concentrations has distinct influence on thermal conductivity and viscosity of nanofluid. Abu-Nada and Chamkha (2010) investigated the problem of steady natural convection heat transfer in a differentially heated enclosure filled with a CuO-EG-Water nanofluid using different variable thermal conductivity and variable viscosity models. Different behaviors (enhancement or deterioration) were predicted in the average Nusselt number as the volume fraction of nanoparticles increases depending on the combination of CuO-EG-water variable thermal conductivity and viscosity models employed. The laminar free convective heat transfer performance and pressure drop of various nanofluids flowing in a straight circular pipe under a constant heat flux condition were numerically studied by Bajestan *et al*. (2011). The results revealed that the particle volume concentration, Brownian motion and aspect ratio of nanoparticles similar to flow Reynolds number increase the heat transfer coefficient, while the nanoparticle diameter has an opposite effect on the heat transfer coefficient. Sundar *et al*. (2013) performed an experimental analysis on the thermal conductivity of ethylene glycol and water mixture based Fe_3O_4 nanofluid. Magnetic Fe_3O_4 nanoparticles were synthesized by chemical co-precipitation method and the nanofluids were prepared by dispersing nanoparticles into different base fluids like 20:80%, 40:60% and 60:40% by weight of the ethylene glycol and water mixture. Their results indicated that the thermal conductivity of nanofluid increases with increase of particle volume concentration and temperature. The same problem was again investigated by Sundar *et al*. (2014) with Al_2O_3 nanoparticle. They found that the maximum thermal conductivity enhancement was observed for 20:80% EG-water nanofluid about 32.26% in the volume concentration of 1.5% at a temperature of 60°C and the maximum viscosity enhancement was observed for 60:40% EG-water nanofluid about 2.58-times in the volume concentration of 1.5% at a temperature of 0° C. Bhanvase *et al*. (2014) presented a study of heat transfer performance of water, ethylene glycol based nanofluids with TiO_2 nanoparticles. They concluded that improving the heat transfer characteristics and compatibility of TiO_2 nanofluid based on EG-water mixture can be a great option in heat transfer equipments. Suganthi *et al*. (2014) carried out an experiment on preparation and characterization of ZnO-EG and ZnO-EG-water nanofluids. It is showed that ZnO-EG and ZnO-EG-water nanofluids had better heat absorption characteristics compared to

Table 1 Summary of results on convective heat transfer of nanofluids

Investigator	Nanofluids	Findings
Wang *et al*. (1999)	CuO/Al_2O_3 dispersed in water, vacuum pump fluid, engine oil and EG	Thermal conductivity of nanofluid mixtures increases with decreasing the particle size
Jang and Choi (2006)	$Cu/Al_2O_3/CuO$-EG /water nanofluid	New correlation for thermal Conductivity $[k_{nf}= (1-\varphi)k_m+\beta_0 k_p \varphi+3C_0 d_m/d_n Pr_T Re^2 k_m \varphi]$
Namburu *et al*. (2007)	CuO-EG-water (binary mixture)	New correlation for viscosity $[Log(\mu s) = Ae^{-BT}]$
Abu-Nada and Chamkha (2010)	CuO/EG-water (binary mixture)	Average Nusselt number increased for volume fraction of nanoparticles
Sundar *et al*. (2013)	Fe_3O_4-EG-water (binary mixture)	Thermal conductivity of nanofluid increased with increase of particle volume concentration and temperature
Tiwari *et al*. (2013a)	$CeO_2/Al_2O_3/TiO_2/SiO_2$-water nanofluid	CeO_2-water nanofluid provided the best performance on heat transfer rate at lower volume concentrations
Tiwari *et al*. (2013b)	CeO_2-water nanofluid	Heat transfer coefficient increased with nanoparticle volume concentration and decreased with temperature
Bhanvase *et al*. (2014)	TiO_2-EG-water (binary mixture)	Heat transfer coefficient increased with increase of volume fraction of nanoparticles
Suganthi *et al*. (2014)	ZnO-EG and ZnO-EG - water(binary mixture)	Heat transfer rate was proportional to thermal conductivity
Sheikholeslami and Rashidi (2015)	Fe_3O_4-water nanofluid	Nusselt number was an increasing function of Ra and nanoparticle volume fraction but decreasing function of Hartmann number
Freidoonimehr *et al*. (2015)	$Cu/CuO/Al_2O_3$ TiO_2-water nanofluid	Cu nanoparticles provided the maximum heat transfer coefficient and largest Nusselt number
Aghaei *et al*. (2016)	CuO-water nanofluid	Average Nusselt number increased with increasing volume fraction of nanoparticles
Purusothaman *et al*. (2016)	Cu/Al_2O_3-water nanofluid	Heat transfer rate increased with increase in solid volume fraction and Ra

their respective base fluids. The enhancements in heat transfer were proportional to thermal conductivity enhancements, which showed that superior thermal conductivity of nanofluids could be used for cooling applications. Bourantas *et al*. (2013) analysed the water-based nanofluid with different thermal conductivity and viscosity models in a square enclosure with the presence of discrete heat source. They found that the temperature of heat source decreases with increase the diameter ratio of minimum to maximum as well as the solid volume fraction of nanoparticles. Hamida and Charrada (2015) presented the results of a numerical study on natural convection in a square enclosure filled with Cu-EG nanofluid in the presence of magnetic fields. It was found that the convection was highly suppressed by the applied magnetic field. Recently Purusothaman *et al*. (2016) investigated the natural convection heat transfer performance on a 3 × 3 array of non-protruding heat source mounted in a nanofluid filled rectangular enclosure. The analysis was performed with different types and concentrations of nanoparticles and a wide range of Rayleigh numbers and the enclosure side aspect ratios. It was found that, the row averaged Nusselt number increases monotonically with increasing the Rayleigh number and the nanoparticle volume fraction irrespective value of enclosure side aspect ratio.

Nanofluid technology is an emerging field in the applications of heat transfer in the past decades. Therefore, influences of various nanofluids on the performance of different geometries compared to their base fluid were tested and a large number of numerical studies can be found in literature [Sharma *et al*. (2015), Tiwari *et al*. (2013a), Tiwari *et al*. (2013b), Sheikholeslami and Rashidi (2015), Freidoonimehr *et al*. (2015), Aghaei *et al*. (2016)]. Summary of investigations of the above literature on convective heat transfer of various nanofluids for different studies are given in Table 1. This shows the lack of literature regarding the nanofluid containing the binary mixture filled in sealed three dimensional enclosures which can withstand very low temperatures motivates us to proceed to the following study. Hence we take this opportunity to investigate numerically the three dimensional enclosure embedded with discrete heat sources filled with Cu-EG-Water nanofluid. In this study different range of aspect ratio of the enclosure, the mixture proportion of Ethylene glycol-water, the solid volume fraction of the nanoparticle along with two different thermal conductivity models are considered for reporting the proper choice of the computation parameters and thermal conductivity models to enhance the heat transfer rate from the heat sources, the current research is extended.

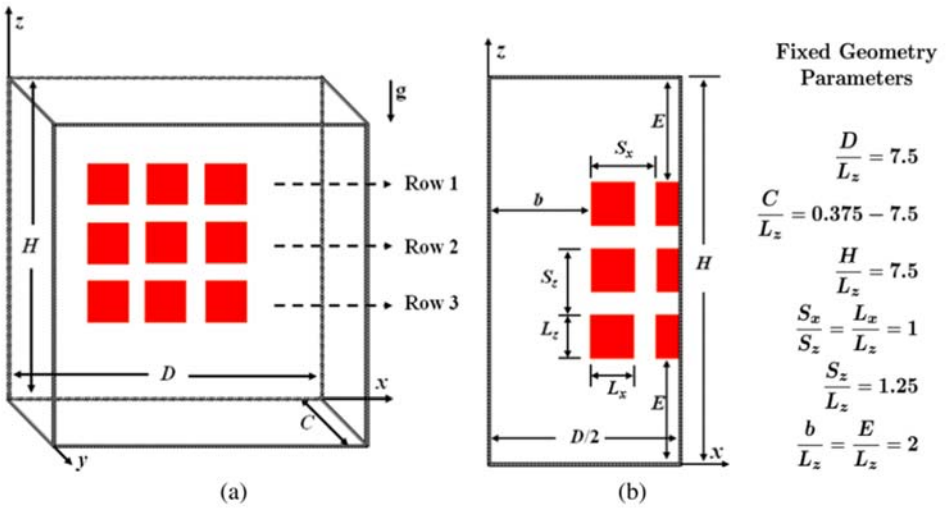

Fig. 1. Physical configuration and Geometric parameters(a) Full view of the enclosure (b) Half view of sources mounted wall at Y=0.

2. MATHEMATICAL FORMULATION

The physical configuration of the system considered in this study and its fixed geometric parameters are shown in Fig. 1. The system consists of three dimensional rectangular enclosure whose height, width and length are denoted by *H, C* and *D* respectively whereas the side aspect ratio of the enclosure is represented by $A_S\ (= H/C)$. On one of the vertical walls ($Y = 0$), a 3 × 3 array of discrete heat sources is mounted and the opposite vertical wall and top wall are assumed to be isothermally cold. On the remaining part of the wall sources are mounted and all other walls are insulated from the surroundings. The enclosure is filled with Cu-EG-water nanofluid mixture containing the basefluids as a mixture of ethylene glycol and water and the nanoparticles Cu. The ethylene glycol and water is mixed in three different ratios namely 20:80, 40:60 and 60:40. The constant thermophysical properties of the nanoparticles, basefluid and mixture of base fluids are listed in Table 2. The flow is three-dimensional, unsteady, laminar incompressible with negligible viscous dissipation and radiation effects. The gravity acts vertically in the downward direction perpendicular to the *XY* plane. The fluid properties are constant except density in the buoyancy term which follows Boussinesq approximation. The governing equations of mass, momentum and energy are cast into non-dimensional form by using the following variables:

$$\begin{aligned} &X = x/L_z,\ \ Y = y/L_z,\ \ Z = z/L_z,\ \ Y = y/L_z,\\ &U = uL_z/\alpha_m,\ V = vL_z/\alpha_m,\ W = wL_z/\alpha_m,\\ &P = pL_z^2/\rho_m\alpha_m^2,\ \theta = (T-T_c)/(T_h-T_c)\\ &Ra = g\beta_m(T-T_c)L_z^3/(\nu_m\alpha_m),\ Pr = \nu_m/\alpha_m. \end{aligned} \tag{1}$$

Hence the governing nondimensional equations [Purusothaman *et al*. (2016)] can be written as:

$$\nabla.\vec{\mathbf{V}} = 0, \tag{2}$$

$$\frac{\partial\vec{\mathbf{V}}}{\partial\tau} + (\vec{\mathbf{V}}.\nabla)\vec{\mathbf{V}} = -\frac{\rho_m}{\rho_{nf}}\nabla P + \frac{\nu_{nf}}{\nu_m}Pr\nabla^2\vec{\mathbf{V}} + \frac{\beta_{nf}}{\beta_m}RaPr\theta\vec{k}, \tag{3}$$

$$\frac{\partial\theta}{\partial\tau} + (\vec{\mathbf{V}}.\nabla)\theta = \frac{\alpha_{nf}}{\alpha_m}\nabla^2\theta, \tag{4}$$

where $\vec{\mathbf{V}}$ is the velocity vector along with the cartesian coordinates *X, Y* and *Z* respectively, ∇^2 is the Laplacian operator and $\vec{\mathbf{k}}$ denotes the unit vector acting along *Z*-direction and the subscript m denotes the mixture of the basefluid and any thermophysical properties of the mixture can be calculated using the formula [Abu-Nada and Chamkha (2010)],

$$\zeta_m = \frac{\xi}{100}\zeta_{EG} + (1-\frac{\xi}{100})\zeta_{water}, \tag{5}$$

Where ζ is the general variable denoting $\rho, c_p, k, \beta, \alpha$ and μ and ξ is the weight percentage of the volume concentration Sundar *et al*. (2013) which can be evaluated as:

$$\xi(\%) = \frac{\left(\frac{W_{EG}}{\rho_{EG}}\right)}{\left(\frac{W_{EG}}{\rho_{EG}}\right)+\left(\frac{W_{water}}{\rho_{water}}\right)}\times 100. \tag{6}$$

The effective density ρ_{nf} and thermal diffusivity α_{nf} of the nanofluid are calculated by

$$\rho_{nf} = (1-\phi)\rho_m + \phi\rho_p, \tag{7}$$

Table 2 Physical properties of nanoparticles and basefluids [Jang and Choi (2006), Abu-Nada and Chamkha (2010)]

Physical property	Water	Ethylene Glycol	Cu-Nano particle	Ethylene Glycol - Water (%)			Nanofluid
				20:80	40:60	60:40	
ρ (kg m^{-3})	997.1	1114	8933	1064.09	1040.79	1018.48	1414.20
Cp (J kg^{-1} K^{-1})	4179	2415	385	3168.01	3519.77	3856.45	2760.06
k (W m^{-1} K-1)	0.613	0.252	400	0.4061	0.4781	0.5469	0.6329
β*10^{-5} (K^{-1})	21	57	1.67	0.4622	0.3744	0.2905	0.2040
α *10^{-7} (m^2 s^{-1})	1.4711	0.9367	1163	1.1648	1.2714	1.3734	1.6216
μ *10^{-2} (Pa s)	0.0909	1.5756	-	0.9040	0.6096	0.3393	0.3857
Pr	6.2	151	-	72.93	46.06	24.25	-

$$\alpha_{nf} = \frac{k_{nf}}{(\rho c_p)_{nf}}, \tag{8}$$

where ϕ is the volume fraction of solid nanoparticles, k_{nf} is the thermal conductivity of the nanofluid and $(\rho c_p)_{nf}$ is the heat capacitance of the nanofluid. In order to discuss the thermal conductivity phenomena, we examine two models proposed theoretically by Maxwell (1904) and Jang and Choi (2006).

The Maxwell model was proposed for thermal conductivity of solid-liquid mixtures with relatively large particles. The thermal conductivity k_{nf} is

$$k_{nf} = \frac{k_p + 2k_m - 2\phi(k_m - k_p)}{k_p + 2k_m + \phi(k_m - k_p)} k_m. \tag{9}$$

An alternative expression for calculating the thermal conductivity of nanofluids was proposed by Jang and Choi (2006). The expression is:

$$k_{nf} = (1-\phi)k_m + \beta_0 k_p \phi + 3C_0 \frac{d_m}{d_p} Pr_T Re^2 k_m \phi, \tag{10}$$

Where β_0 is the Kapitza resistance, $C_0 = 18 \times 10^6$ is a proportional constant, d_m is the diameter of the base fluid, d_p is the diameter of the nanoparticle, Pr_T is thermal Rayleigh number and $Re(=\frac{C_{R,M} d_p}{v})$ is Reynolds number. The instantaneous velocity of the nanoparticle can be defined by $C_{R,M} = \frac{D_0}{l_m}$, where D_0 is the microscopic diffusion coefficient and l_m is the free mean path of the basefluid; also D_0 is defined by $D_0 = \frac{k_m T}{3\pi\mu_m d_p}$ In addition, the specific heat capacitance and thermal expansion coefficient are calculated by

$$(\rho c_p)_{nf} = (1-\phi)(\rho c_p)_m + \phi(\rho c_p)_p, \tag{11}$$

$$(\rho\beta)_{nf} = (1-\phi)(\rho\beta)_m + \phi(\rho\beta)_p, \tag{12}$$

and the dynamic viscosity of the nanofluid μ_{nf} can be approximated using the Brinkman (1952) relation.

$$\mu_{nf} = \frac{\mu_m}{(1-\phi)^{2.5}}. \tag{13}$$

The dimensionless boundary conditions maintained at the enclosure walls are

$$\begin{aligned}
&\text{At } X = 0, \frac{D}{L_z}: U = V = W = 0, \ \frac{\partial\theta}{\partial X} = 0, \\
&\text{At } Y = 0: U = V = W = 0, \begin{cases} \theta = 1, & \text{source region} \\ \frac{\partial\theta}{\partial X} = 0, & \text{otherwise} \end{cases} \\
&\text{At } Y = \frac{C}{L_z}: U = V = W = 0, \ \theta = 0, \\
&\text{At } Z = 0: U = V = W = 0, \ \frac{\partial\theta}{\partial Z} = 0, \\
&\text{At } Z = \frac{H}{L_z}: U = V = W = 0, \ \theta = 0.
\end{aligned} \tag{14}$$

Tou *et al*. (1999) discussed the plane of symmetry in their three dimensional natural convection problem and this assertion was experimentally confirmed by Ozoe *et al*. (1979). Following this, the plane at $X = D / 2L_z$ is taken as a plane of symmetry and the computational domain is reduced by half. The symmetric boundary conditions imposed on the walls are another important factor which ensure the possibility of taking half of the domain for computation; hence it can be defined as follows:

$$\text{At X}=\frac{D}{2L_z}: \ U = \frac{\partial V}{\partial X} = \frac{\partial W}{\partial X} = 0, \ \frac{\partial\theta}{\partial X} = 0. \tag{15}$$

The heat transfer rate within the enclosure can be acquired through the Nusselt number. The local and average Nusselt numbers are calculated from the resulting temperature field at each heat source and are defined as follows:

The local Nusselt number

$$Nu_{i,k}(X,Z) = \frac{k_{nf}}{k_m}\frac{\partial\theta}{\partial Y}, \tag{16}$$

the average Nusselt number

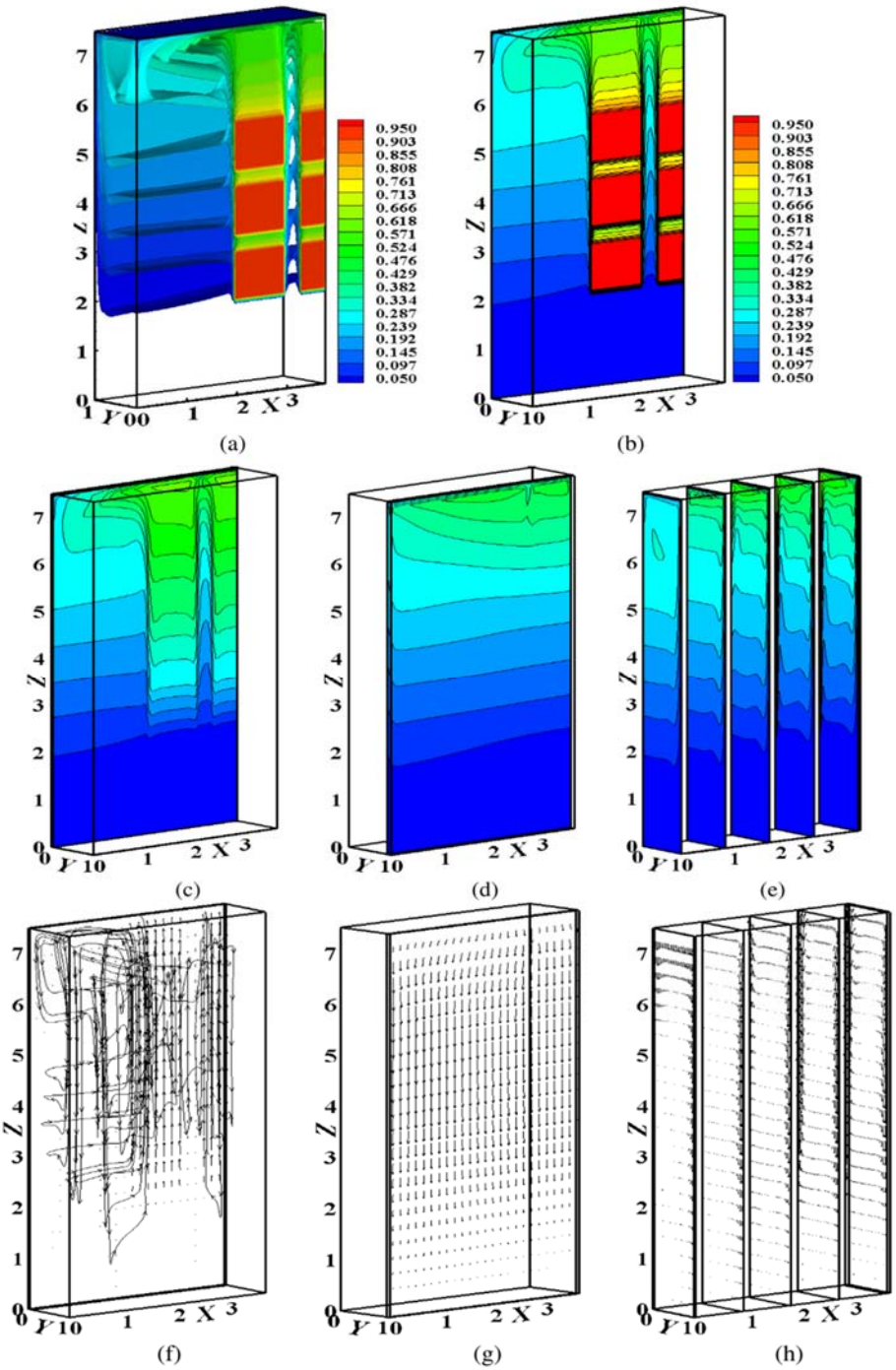

Fig. 2. Model 2; (a) Isothermal surfaces, Isotherms at (b) Y = 0, (c) Y = 0.05 (d) Y = 0.9 (e) X = 1.0, 2.0, & 3.0; Velocity vector at (f) Y = 0.05 (g) Y = 0.9 (h) X = 1.0, 2.0, and 3.0. for Cu-EG-water nanofluid (EG-water proportion - 40:60) with ϕ = 0.05, A_S = 7.5.

$$\overline{Nu}_{i,k}(X,Z)=\frac{1}{A_h}\int_0^{A_h} Nu_{i,k}(X,Z)dA_h, \tag{17}$$

the row averaged Nusselt number

$$\overline{Nu}_i=\frac{1}{3}\sum_{i=1}^{3}\overline{Nu}_{i,k}(X,Z), \tag{18}$$

where A_h is the heater area and the subscripts *i,k* refer to the specified heaters in row *i* and column *k*.

3. NUMERICAL PROCEDURE

The governing nondimensional equations (2)-(4)

have been solved numerically based on finite volume technique as described by Patankar (1980). A uniform staggered grid is considered in the computational domain. That is the scalar quantities (P and θ) are stored in the nodal points whereas the components of the velocity (U,V and W) are stored at the cell face of the control volumes of the nodal points. A fully implicit time marching scheme is employed. The numerical procedure namely Semi-Implicit Method for Pressure Linked Equation (SIMPLE) algorithm is used to handle the pressure velocity coupling. The convective and diffusive terms in equations (2)-(4) are handled by adopting the power law scheme. The discretized form of the Eq.(3) can be written as

$$\frac{\varphi-\varphi_P^0}{\Delta\tau}\Delta V+[(\varphi U)_e-(\varphi U)_w]\Delta Y\Delta Z+[(V\varphi)_e-(V\varphi)_w]\Delta X\Delta Z+[(W\varphi)_e-(W\varphi)_w]\Delta X\Delta Z=\Gamma^{\varphi}\left[\left(\frac{\partial\varphi}{\partial X}\right)_e-\left(\frac{\partial\varphi}{\partial X}\right)_w\right]\Delta Y\Delta Z+\Gamma^{\varphi}\left[\left(\frac{\partial\varphi}{\partial Y}\right)_n-\left(\frac{\partial\varphi}{\partial Y}\right)_s\right]\Delta X\Delta Z+\Gamma^{\varphi}\left[\left(\frac{\partial\varphi}{\partial Z}\right)_t-\left(\frac{\partial\varphi}{\partial Z}\right)_b\right]\Delta X\Delta Y+S^{\varphi}(X,Y,Z). \quad (19)$$

The Power law scheme is employed to minimize the numerical diffusion for the convective terms to the discretized Eq.(19) to obtain the form

$$a_P\varphi_P=a_E\varphi_E+a_W\varphi_W+a_N\varphi_N+a_S\varphi_S+a_T\varphi_T+a_B\varphi_B+S^{\varphi}(X,Y,Z).$$

Where

$$a_E=D_e max[0,(1-0.1|pe_e|^5]+max[-F_e,0]$$
$$a_W=D_w max[0,(1-0.1|pe_w|^5]+max[-F_w,0]$$
$$a_N=D_n max[0,(1-0.1|pe_n|^5]+max[-F_n,0]$$
$$a_S=D_s max[0,(1-0.1|pe_s|^5]+max[-F_s,0]$$
$$a_T=D_t max[0,(1-0.1|pe_t|^5]+max[-F_t,0]$$
$$a_B=D_b max[0,(1-0.1|pe_b|^5]+max[-F_b,0]$$
$$a_P=a_E+a_W+a_N+a_S+a_T+a_B+a^0p.$$

Finally, the discretized set of algebraic equations are solved by the line-by-line Tri-Diagonal Matrix Algorithm (TDMA). To ensure convergence of the numerical algorithm, the following criterion is applied to all dependent variables over the solution domain

$$\frac{\sum_{i,j,k}|\varphi_{i,j,k}^n-\varphi_{i,j,k}^{n-1}|}{\sum_{i,j,k}|\varphi_{i,j,k}^n|}\le 10^{-5} \quad (20)$$

where φ represents the dependent variables *U,V,W* and θ, the subscripts *i,j,k* indicate the space co-ordinates and the superscript n represents the time step. Based on the above numerical procedure, the present problem is solved by the developed FORTRAN code. The computations were performed on the Dell Precision T3400 workstation and the typical computational time is around three to four days for a productive run. The authors have already employed the above solution methodology used for this study in our previous paper [Purusothaman *et al*. (2016)] and hence the reader can refer it for numerical validation and comparison with other results in the literature.

In order to examine the effect of the grid on the numerical study, the numerical code was examined for Model 1 (20:80) with $Ra = 10^7$, $\phi = 0.05$ and $A_S = 7.5$. The row averaged Nusselt numbers $\overline{Nu}_i, i = 1, 2$ and 3 for Row 1, Row 2 and Row 3 are calculated using five different computational grids, namely, 55×31×91, 61×31×91, 76×91×91, 91×91×91 and 109×91×121. The results are given in Table 3 and it is observed that a refinement of the grid from 91×91×91 to 109×91×121 does not have a significant effect on the results in terms of row average Nusselt number. Hence by considering both the accuracy and computational time, the present calculations are all performed with a 91×91×91 spaced grid system.

4. RESULTS AND DISCUSSION

A comprehensive study of three dimensional natural convection cooling of a 3 × 3 array of discrete heaters in a rectangular enclosure using Cu-EG-water nanofluid is numerically investigated. For this study, the computations are performed for a wide range of enclosure side aspect ratio A_S (1.0, 2.0, 7.5), mixture proportion of Ethylene glycol and water (20:80, 40:60, 60:40) and solid volume fractions of Cu nanoparticles ϕ (0.0, 0.05, 0.1) along with two different thermal conductivity models. The Rayleigh number is kept fixed at Ra = 10^7 throughout the computation. The effect of heat transfer and fluid flow performance on isothermal surfaces, isotherms and velocity vectors; the effect of average Nusselt number on enclosure side aspect ratio, mixture proportion of Ethylene glycol-water, solid volume fractions of Cu nanoparticles and comparison among two different thermal conductivity models on heat transfer performance are presented and discussed.

4.1 3-D nature of Temperature and flow Field

Figure. 2 illustrates the isothermal surfaces, isotherms and vector vectors at selected plane sections corresponding to Model-2 for the fixed value of enclosure side aspect ratio $A_S = 7.5$ and solid volume fraction □ = 0.05. The ratio of ethylene glycol-water is fixed to be 40:60% in weight. It is found from Figs. 2(a)-(e) that the entire region lying below the bottom row of heaters remains convectively inactive and the heat transfer trend in this region is dictated by conduction alone. However it is noticed that the isotherms are tightly packed with the heat sources which are quantitatively expressing

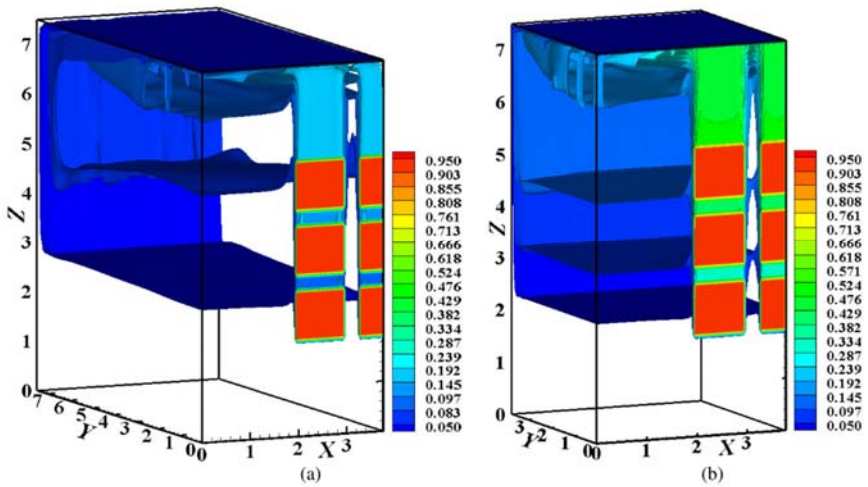

Fig. 3. Model 2; Isothermal surfaces (a) A_S = 1.0 (b) A_S = 2.0 for Cu-EG-water nanofluid (EG-water proportion - 40:60) with ϕ = 0.05.

Table 3 Grid Study for Model-1(20:80) with Ra = 10^7 and AS = 7.5, ϕ= 0:05

Grids	$\overline{NU_3}$	$\overline{NU_2}$	$\overline{NU_1}$
55× 31×91	36.9890	25.7792	20.9693
61×31×91	36.7245	25.5648	20.6892
76×91×91	36.5942	25.2975	20.3568
91×91×91	36.4648	24.8270	19.9451
109×91×121	36.4647	24.8268	19.9449

the convection mechanism remains significantly active well on the heater array. Isothermal surfaces originating from the heat sources reach the opposite cold wall in the form of wavy surfaces (See Fig. 2 (a)), but adjacent to the top cold ceiling, a very complex flow pattern is developed due to the non uniformity in downward flows. The magnitude of the velocity vectors adjacent to the column heaters is maximum due to enormous energy generated by the discrete heaters. The path of the fluid flow is clearly predicted by the stream traces (Fig. 2(f)) where the bulk fluid motion driven by the buoyancy force moves rapidly upwards and loses its momentum due to the cooled top and falls down freely near the opposite and adjacent walls of the enclosure. Adjacent to the opposite cold wall at Y = 0.9, the majority of the fluid motion is vertically downward. Further the fluid gets interacted with the array of heaters and the process continues by forming a helical flow pattern inside. However the fluid in the bottom region of the enclosure is practically stagnant since the region is convectively inactive.

4.2 Effect of Enclosure Side Aspect Ratio

In these simulations, the effect of enclosure side aspect ratio is an important factor to be considered to obtain the configuration with more thermal efficiency and the results are displayed in Figs. 3 and 4. Fig 3(a) and (b) represent the isothermal surfaces for A_S = 1.0 and 2.0 respectively for Model-2 with fixed EG-water proportion (40:60) and ϕ = 0.05. It is observed that the thermal plumes over the heater columns ascend upwards and develops weak circulation near the top cold ceiling for A_S = 1.0. The bottom part of the enclosure is almost stagnant. Moreover, it is noticed that as the enclosure side aspect ratio A_S (=2.0) increases, the circulation induced by the heaters also increases and develops a complex flow pattern. When A_S is increased the isotherms get crowded near the ceiling and starts descending. This is due to the fact that the top cold surface area decreases when A_S increases.

Isotherms at adiabatic planes (X = 0.0 and 3.75) for Model-2 with ϕ = 0.05, A_S = 1.0-7.5 for Cu-EG-water nanofluid (EG-water proportion-40:60) are shown in Fig. 4. It is noticed that the closed loops with local maximum temperature are found on the top of side adiabatic wall due to the non-uniform downward flows from the ceiling. One of the main interesting applications in the study of cooling of electronic equipments is that of finding the hot spots on the enclosure walls. Therefore much attention is

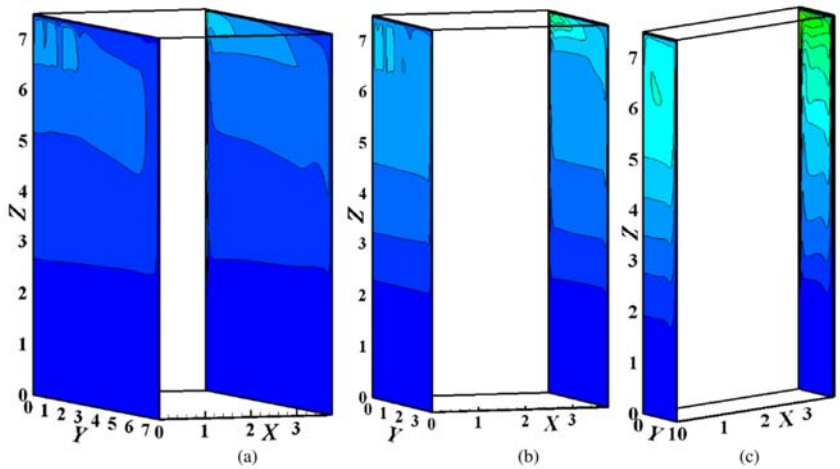

Fig. 4. Model 2; Isotherms at X = 0.0 & 3.75 planes (a) A_S = 1.0 (b) A_S = 2.0 (c) A_S = 7.5 for Cu-EG-water nanofluid (EG-water proportion - 40:60) with ϕ = 0.05.

paid to predict the closed loops with local maximum temperature on the adjacent walls of the heater mounted walls. These loops gained a special attention in the field of inducing passive cooling of electronic equipments and hence by keeping sinks at this hot loops, thus providing a pathway to reduce the temperature within the enclosure.

4.3 Heat Transfer

In order to view the detailed discussion on different behaviors of the heat transfer performance driven throughout the three dimensional enclosure, the average Nusselt number over the 3×3 array of discrete heaters is calculated. The bargraph shown in Fig. 5 is used to differentiate the two different models of thermal conductivity, namely, Maxwell-Garnett Model (Fig. 5(a)) and Jang and Choi Model (Fig. 5(b)). Three different side aspect ratios of the enclosure are taken into consideration and the mixture proportion of Ethylene glycol and water is also varied to find the suitable combination which results in the enhanced heat transfer and better thermal cooling activity. In the absence of nanoparticles, the upcoming convective stream makes the maximum heat transfer rate at the bottom row heaters that gets minimized as it moves towards the top row heaters, that is, $\overline{Nu}_1 < \overline{Nu}_2 < \overline{Nu}_3$. We can also notice the increasing heat transfer rate for increasing aspect ratio and this is true only for bottom row heaters while for the top two rows of heaters it exhibits a maximum value of Nusselt number at A_S = 2.0. The above effect is maintained for all values of volume concentrations of nanoparticles.

Increasing solid volume fraction of nanoparticles is another important factor in the determination of thermal activity and it shows a great augmentation in transferring the heat away from the heaters. The heat transfer rate is increased for an increasing values of solid volume fraction of nanoparticles. The effect of ratio of ethylene glycol to water in Model-1 failed to show a significant change because it depends only on the solid volume fraction. But Model-2 deals with all the main features like solid volume fraction, diffusion coefficient, diameter of both the nanoparticle and basefluid, mean free path of the nanoparticle which are the key factors in revealing the thermal conductivity of the nanofluid. When the ratio of EG-water mixture is fixed to be 60:40, the row average Nusselt number attains its maximum value compared with the other two ratios. It is also predicted that the heat transfer rate increases with increasing values of the nanoparticles volume fraction using the Model-2 than Model-1.

5. CONCLUSION

Buoyancy induced natural convection in a three dimensional enclosure with an array of discrete heaters is numerically investigated. A 3 × 3 array of non-protruding heat sources is embedded on one of the vertical walls of the enclosure while the top horizontal and opposite vertical walls are assumed to be isothermally cold. The enclosure is filled with composition of two different base fluids with dispersed Cu-nanoparticles. The important conclusions obtained in this study are listed below:

- Among the two different thermal conductivity models, Model-2 yields a fruitful result by achieving better thermal performance than Model-1, since Model-2 depends on the significant characteristics like diffusion coefficient, diameter of both the nanoparticle and basefluid and mean free path.
- By increasing solid volume fraction of the nanoparticles and fixing the aspect ratio at 2.0, the maximum heat transfer rate is obtained.
- The significant average Nusselt number is obtained when the ratio of Ethylene Glycol and water is in the percentage of 60 and 40 respectively.

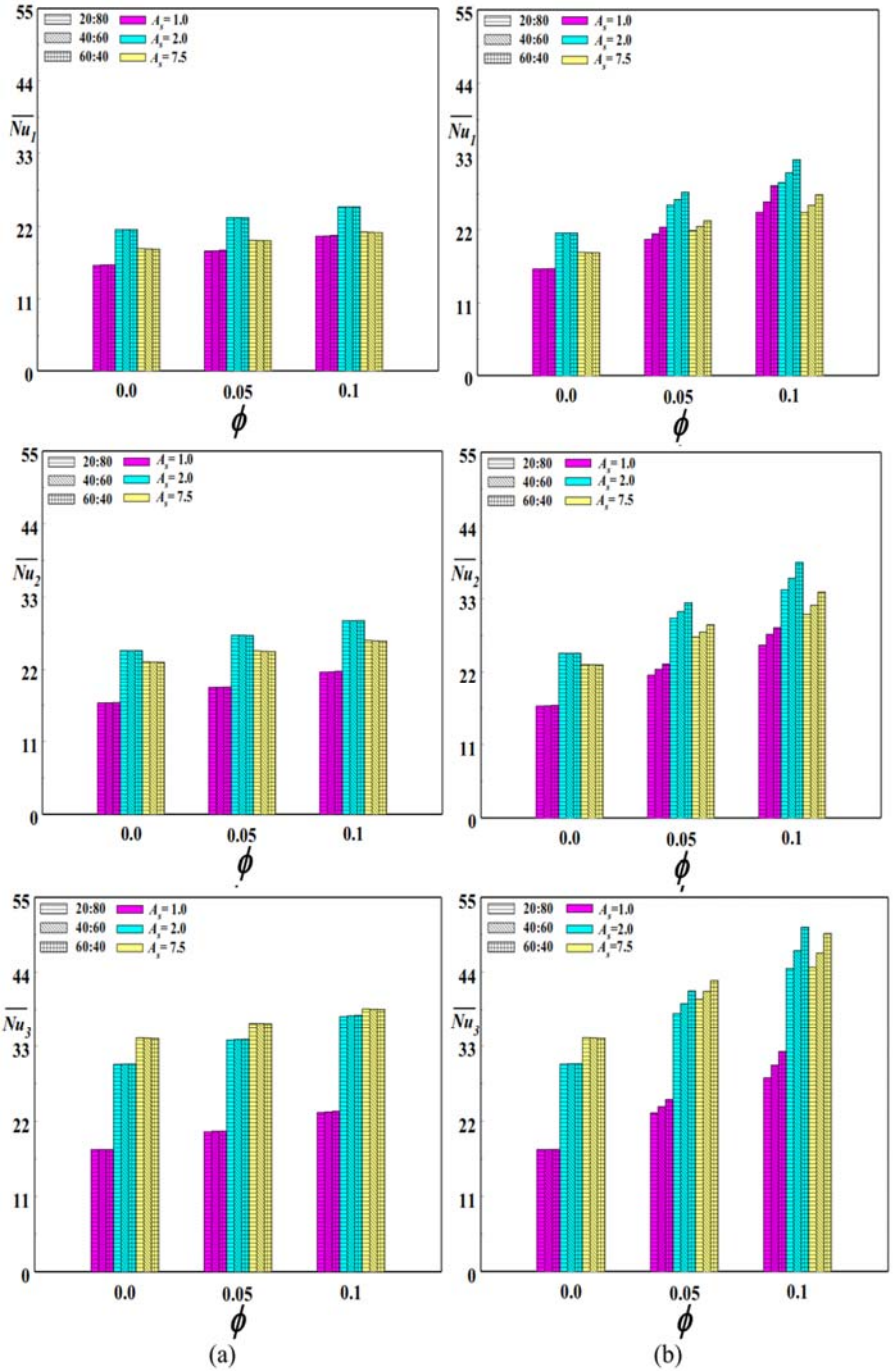

Fig. 5. Effect of average Nusselt number against different volume fraction of nanoparticles, (a) Model-1 (b) Model - 2.

REFERENCES

Abu-Nada, E. and A. Chamkha (2010). Effect of nanofluid variable properties on natural convection in enclosures filled with a CuO-EG-water nanofluid. *International Journal of Thermal Sciences* 49(12), 2339-2352.

Aghaei, A., A. Abbasian Arani and F. Abedi (2016). Analysis of magnetic field effects on distributed heat sources in a nanofluid-filled enclosure by natural convection. *Journal of Applied Fluid Mechanics* 9(3), 1175-1187.

Bajestan, E., H. Niazmand, W. Duangthongsuk and S. Wongwises (2011). Numerical investigation of effective parameters in convective heat transfer of nanofluids flowing under a laminar

flow regime. *International Journal of Heat and Mass Transfer* 54(19), 4376-4388.

Bhanvase, B., M. Sarode, L. Putterwar, K. Abdullah, M. Deosarkar and S. Sonawane (2014). Intensification of convective heat transfer in water/ethylene glycol based nanofluids containing TiO_2 nanoparticles. *Chemical Engineering and Processing: Process Intensification* 82, 123-131.

Bourantas, G., E. Skouras, V. Loukopoulos and G. Nikiforidis (2013). Natural convection of nanofluids flow with "nanofluid-oriented" models of thermal conductivity and dynamic viscosity in the presence of heat source. *International Journal of Numerical Methods for Heat and Fluid Flow* 23(2), 248-274.

Brinkman, H. (1952). The viscosity of concentrated suspensions and solutions. *Journal of Chemical Physics* 20(4), 571-581.

Choi, S. and J. Eastman (1995). Enhancing thermal conductivity of fluids with nanoparticles. *Developments and Applications of Non-Newtonian flows, ASME* 231(2), 99-105.

Freidoonimehr, N., M. Rashidi and S. Mahmud (2015). Unsteady MHD free convective flow past a permeable stretching vertical surface in a nanofluid. *International Journal of Ther-mal Sciences* 87, 136-145.

Hamida, M. and K. Charrada (2015). Natural convection heat transfer in an enclosure filled with an Ethylene Glycol - Copper nanofluid under magnetic fields. *Numerical Heat Transfer, Part A: Applications* 67(8), 902-920.

Jang, S. and S. Choi (2006). Effects of various parameters on nanofluid thermal conductivity. *ASME. Journal of Heat Transfer* 129(5), 6170-623.

LotfizadehDehkordi, B., S. Kazi, M. Hamdi, A. Ghadimi, E. Sadeghinezhad and H. Metselaar (2013). Investigation of viscosity and thermal conductivity of alumina nanofluids with addition of SDBS. *Heat Mass Transfer* 49(8), 1109-1115.

Maxwell, J. (1904). *A Treatise on Electricity and Magnetism*. Cambridge, Oxford University Press, UK.

Namburu, P., D. Kulkarni, D. Misra and D. Das (2007). Viscosity of copper oxide nanoparticles dispersed in ethylene glycol and water mixture. *Experimental Thermal and Fluid Science* 32(2), 397-402.

Ozoe, H., N. Sato and S. Churchill (1979). Experimental confirmation of the three dimensional helical streaklines previously computed for natural convection in inclined rectangular enclosures. *International Chemical Engineering* 19(3), 454-462.

Patankar, S. (1980). *Numerical Heat Transfer and Fluid Flow*. Hemisphere Publishing Corporation, New York.

Purusothaman, A., N. Nithyadevi, H. Oztop, V. Divya, and K. Al-Salem (2016). Three dimensional numerical analysis of natural convection cooling with an array of discrete heaters embedded in nanofluid filled enclo-sure. *Advanced Powder Technology* 27(1), 268-280.

Sharma, K., K. Kaushalyayan and M. Shukla (2015). Pull-out simulations of interfacial properties of amine functionalized multi-walled carbon nanotube epoxy composites. *Computational Materials Science* 99, 232–241.

Sheikholeslami, M. and M. Rashidi (2015). Effect of space dependent magnetic field on free convection of Fe_3O_4-water nanofluid. *Journal of the Taiwan Institute of Chemical Engineers* 56, 6–15.

Suganthi, K., V. Vinodhan, and K. Rajan (2014). Heat transfer performance and transport properties of ZnO-ethylene glycol and ZnO-ethylene glycol-water nanofluid coolants. *Applied Energy* 135, 548-559.

Sundar, L., E. Venkata Ramana, M. Singh, and A. Sousa (2014). Thermal conductivity and viscosity of stabilized ethylene glycol and water mixture Al_2O_3 nanofluids for heat transfer applications: An experimental study. *International Communications in Heat and Mass Transfer* 56, 86-95.

Sundar, L., M. Singh and A. Sousa (2013). Thermal conductivity of ethylene glycol and water mixture based Fe_3O_4 nanofluid. *International Communications in Heat and Mass Transfer* 49, 17-24.

Tiwari, A., P. Ghosh and J. Sarkar (2013a). Heat transfer and pressure drop characteristics of CeO_2 /water nanofluid in plate heat exchanger. *Applied Thermal Engineering* 57, 24-32.

Tiwari, A., P. Ghosh and J. Sarkar (2013b). Performance comparison of the plate heat exchanger using different nanofluids. *Experimental Thermal and Fluid Science* 49, 141-151.

Tou, S., C. Tso and X. Zhang (1999). 3-D numerical analysis of natural convective liquid cooling of a 3 × 3 heater array in rectangular enclosures. *International Journal of Heat and Mass Transfer* 42(17), 3231-3244.

Trisaksri, V. and S. Wongwises (2007). Critical review of heat transfer characteristics of nanofluids. *Renewable and Sustainable Energy Reviews* 11(3), 512–523.

Wang, X. and A. Mujumdar (2007). Heat transfer characteristics of nanofluids: a review. *International journal of thermal sciences* 46(1), 1-19.

Wang, X., X. Xu and S. Choi (1999). Thermal conductivity of nanoparticle-fluid mixture. *Journal of thermophysics and heat transfer* 13(4), 474-480.

)16.